

Topological Weyl and Node-Line Semimetals in Ferromagnetic Vanadium-Phosphorous-Oxide β -V₂OPO₄ Compound

Y. J. Jin^{1,*}, R. Wang^{1,2,*}, J. Z. Zhao^{1,3}, Z. J. Chen^{1,4}, Y. J. Zhao⁴, and H. Xu^{1,†}

¹*Department of Physics, South University of Science and Technology of China, Shenzhen 518055, P. R. China.*

²*Institute for Structure and Function & Department of physics, Chongqing University, Chongqing 400044, P. R. China.*

³*Dalian Institute of Chemical Physics, Chinese Academy of Sciences, 116023 Dalian, P. R. China and*

⁴*Department of Physics, South China University of Technology, Guangzhou 510640, P. R. China*

We propose that the topological semimetal features can co-exist with ferromagnetic ground state in vanadium-phosphorous-oxide β -V₂OPO₄ compound from first-principles calculations. In this magnetic system with inversion symmetry, the direction of magnetization is able to manipulate the symmetric protected band structures from a node-line type to a Weyl one in the presence of spin-orbital-coupling. The node-line semimetal phase is protected by the mirror symmetry with the reflection-invariant plane perpendicular to magnetic order. Within mirror symmetry breaking due to the magnetization along other directions, the gapless node-line loop will degenerate to only one pair of Weyl points protected by the rotational symmetry along the magnetic axis, which are largely separated in momentum space. Such Weyl semimetal phase provides a nice candidate with the minimum number of Weyl points in a condensed matter system. The results of surface band calculations confirm the non-trivial topology of this proposed compound. This findings provide a realistic candidate for the investigation of topological semimetals with time-reversal symmetry breaking, particularly towards the realization of quantum anomalous Hall effect in Weyl semimetals.

Quantum-Hall-effect (QHE) offered us a different pathway to achieve dissipationless current beyond superconductors [1]. However, the potential applications of QHE are strongly limited by the required external high-intensity magnetic fields [2, 3]. An alternative option is the Quantum-spin-Hall (QSH) insulators that works independently with respect to external magnetic fields but, unfortunately, will be suppressed when the sample size become larger than a critical value due to the existence of non-elastic scattering between states with opposite directions in helical edge states [4–6]. The most promising solution of these challenges is the proposed quantum-anomalous-Hall (QAH) materials with intrinsic long-rang magnetic order that are able to be free for any sample-size or external field [7–9].

To achieve this, magnetic topological materials, including topological insulators (TIs) [7–11] and topological semimetals (TSMs)[12] in their quantum-well structure with time-reversal (TR) symmetry breaking, have attracted intensive attention recently. Distinguished from gaped magnetic TIs, magnetic TSMs, i.e. spin polarized Weyl and node-line semimetals, host finite numbers (Weyl) or continues distributed (node-line) band crossing points near the Fermi level in momentum space. Such crystal symmetry protected features lead exotic conductive surface states, which are Fermi arcs in Weyl semimetals (WSMs) [13] and drumhead states in node-line semimetals (NLSs) [14]. Accomplishing these robust spin dependent surface states is the key step of achieving several unusual spectroscopic and transport phenomena especially the QAH in their quantum-well structure experimentally.

Up to now, the non-magnetic TSMs have been stud-

ied intensively [15–25], but only a few magnetic TSMs have been proposed. For instance, magnetic HgCr₂Se₄ has been predicted to host only two nodal points [12] which is defined as a Chern semimetal, not fully fit the WSM features since each crossing points possessing chiral charge of 2. So far, nontrivial properties in HgCr₂Se₄ have not been verified experimentally due to the requirement of large magnetic domains [26, 27]. Very recently, Co-based magnetic Heusler alloys were also predicted to host the topology of WSMs [28]. However, the energy of Weyl points is much higher above the Fermi level (~ 0.6 eV). Therefore, additional tuning of the energy of Weyl points relative to Fermi level is necessary [28] for future applications.

In this work, we propose that the ferromagnetic (FM) vanadium-phosphorous-oxide β -V₂OPO₄, a potential material for lithium-ion battery [29, 30], presents either NL or WSM features that can be easily switched by different magnetization directions. The node-line band structures, in $D_{4h}(C_{4h})$ magnetic group with spin-orbital coupling (SOC), are protected by the mirror reflection symmetry with the reflection-invariant plane perpendicular to the spin-polarized direction. This gapless node-line loop, which lies in the reflection-invariant plane and very close to the Fermi level, will degenerate to two large separated Weyl points protected by rotational symmetry in the same plane once mirror reflection symmetry is broken due to the magnetization along other directions. In these cases, the system host the minimum number of Weyl points. Based on our first-principles calculations, this non-trivial FM β -V₂OPO₄ is a promising candidate of experimentally studying on magnetic TSMs.

We perform the first-principles calculations using the

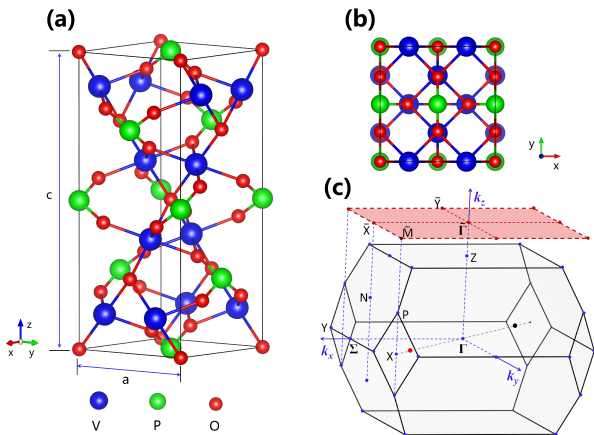


FIG. 1. Crystal structure and Brillouin zone (BZ). The side (a) top (b) view of crystal structure of β - V_2OPO_4 with the space group $I4_1amd$ (No. 141). V, P, and O atoms are indicated by blue, green, and red spheres, respectively. (c) The body-centered-tetragonal (BCT) BZ and the corresponding (001) surface BZ. The high symmetry points are also indicated. Two Weyl points with opposite chirality are symmetrically located at Γ -X axis as red ($C = +1$) and black ($C = -1$) dots, with a magnetization along the $[110]$ direction.

Vienna *ab initio* Simulation Package (VASP) [31, 32] based on density functional theory [33, 34]. For the exchange-correlation potential we choose the generalized gradient approximation (GGA) with the Perdew-Burke-Ernzerhof (PBE) formalism [35, 36]. The core-valence interactions are treated by the projector augmented wave (PAW) method [37–39]. A plane-wave-basis set with kinetic-energy cutoff of 600 eV has been used. The full Brillouin zone (BZ) is sampled by $21 \times 21 \times 21$ Monkhorst-Pack grid to simulate the electronic behaviors [40]. Due to the strongly correlated effects of $3d$ electrons in vanadium, GGA+U calculations is necessary to describe the on-site Coulomb repulsion beyond the GGA pictures [41, 42]. We notice that the band inversion has been confirmed in a large range of U in β - V_2OPO_4 from 1.5 eV to 10.0 eV. In this work, the effective on-site Coulomb energy U is chosen to be 3.0 eV to illustrate the band topology, which works well in fitting the properties of vanadium-oxide system [43]. To calculate the surface states and Fermi arcs, the tight-binding Hamiltonian is constructed by projecting the Bloch states into maximally localized Wannier functions [44, 45].

As it is illustrated in Figs. 1(a) and (b), the vanadium-phosphorous-oxide β - V_2OPO_4 compound crystallizes in body-centered-tetragonal (BCT) structure with a space group $I4_1amd$ (No. 141). Structural optimization obtains the calculated lattice constants which are $a = 5.465$ Å and $c = 12.544$ Å, in nice agreement with experimental values $a = 5.362$ Å and $c = 12.378$ Å [46]. The O atoms take two Wyckoff positions $4a$ (0.0, 0.0, 0.0) and

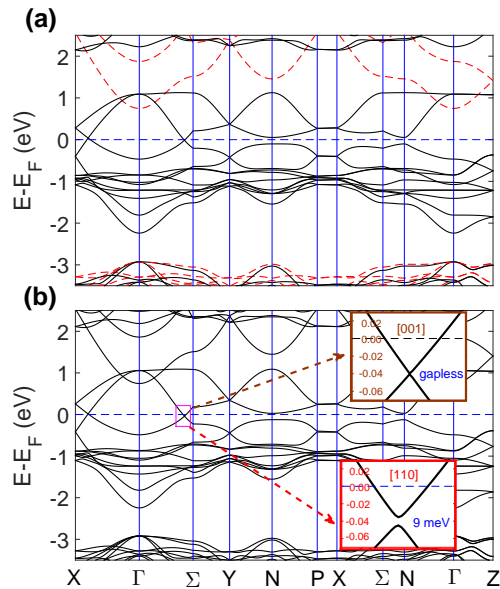


FIG. 2. (a) The band structures of β - V_2OPO_4 along high-symmetry lines without spin-orbital coupling (SOC), and the majority and minority spin bands are denoted by the solid (black) and dashed (red) lines, respectively. (b) The SOC band structures. The upper and lower insets respectively represent the bands with the $[001]$ and $[110]$ magnetism in Γ - Σ direction.

$16h$ (0.00000, 0.23762, 0.43299). The P and V atoms are located at Wyckoff positions $4b$ (0.0, 0.0, 0.5) and $8c$ (0.250, 0.000 0.875), respectively. The BCT BZ and corresponding (001) surface BZ are shown in Fig. 1(c), in which high-symmetry points are marked.

Our results confirm the FM groundstate of β - V_2OPO_4 , which is about 86 meV lower than the antiferromagnetic state per unit cell, with magnetic moment $\sim 2.5 \mu_B$ per V atom. The electronic band structures in the absence of SOC [see Fig. 2(a)] show that the spins and orbitals are independent and two spin channels are decoupled around the Fermi level. These two spin channels present different electronic states, i.e. a ~ 3.68 eV band gap of the minority spin states and the semimetallic features of majority spin states, indicating the half-metallic properties of the system. The band crossings reveals around Γ point in the $k_z = 0$ plane, giving rise to a symmetry protected nodal-line loop. These two crossing bands belong to the states that has opposite eigenvalues ± 1 of mirror reflection symmetry operation M_z , respectively, which protects the nodal ring in k_x - k_y plane with $k_z = 0$ [15]. The spin-polarized nodal ring shows a tiny dispersion, the maximum and minimum of which are in the Γ -X and Γ - Σ directions, respectively, i.e. ~ 12 meV higher and ~ 36 meV lower than the Fermi level E_F .

As we report in Fig. 2(b), the SOC little influences on

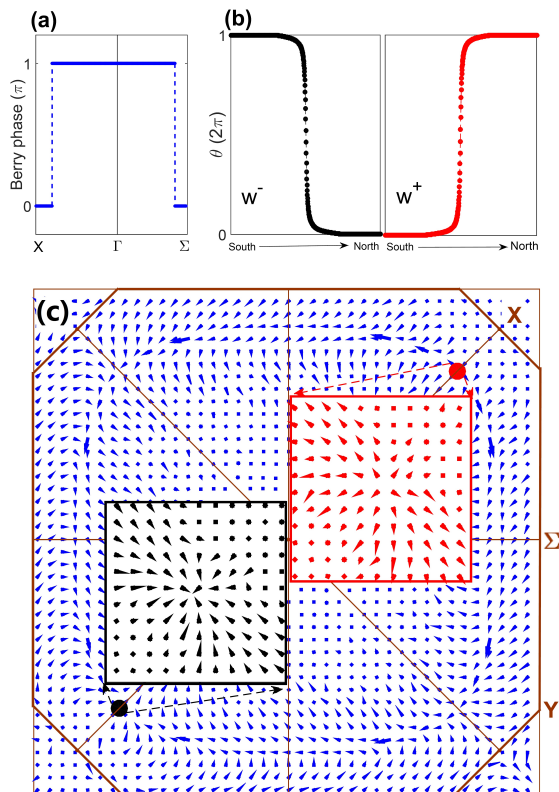


FIG. 3. (a) With magnetization direction along [001] axis, variation of the Berry phase along high-symmetry lines in $k_z = 0$ plane. With magnetization direction along [110] axis, (b) the evolution of average position of Wannier centers obtained by the Wilson-loop method applied on a sphere that encloses on a Weyl point. The average Wannier center shifts downwards from south to north, indicating to negative chirality W^- . The average Wannier center shifts upwards from south to north, indicating to positive chirality W^+ . (c) The distribution of Berry curvature for the $k_z = 0$ plane. The red and black regions denote the Weyl points with negative and positive chirality, respectively.

the band structures in which the half-metallic ferromagnetism remains. The spontaneous magnetization direction is determined by studying the total energy of system with magnetization along different high symmetry axis. The [001] axis is found to be the energetically most favorable magnetization direction. It is worth to mention that, results show very small energy differences, below 0.3 meV, among all magnetic configurations. This implies that the switching between each configurations by external magnetic field would be easy. In the presence of SOC, the magnetic symmetry is dependent on the direction of magnetization. We will respectively present the topological features of the two typical [001] and [110] magnetisms in the following.

When magnetization is polarized along [001] direction, the system reduces to point group C_{4h} , the subgroup of

D_{4h} , in which the fourfold rotation C_4^z is tensored by the inversion I , namely $C_4^z \otimes I$. This magnetic group contains eight irreducible symmetry operators: inversion I , fourfold rotation C_4^z , the product of time reversal T , twofold rotations of C_2 symmetry axes [100], [010], [110], $[1\bar{1}0]$, and the product (IC_2^z) of inversion and rotation C_2^z . The group element IC_2^z is equivalent to the mirror reflection symmetry corresponding to the $x - y$ plane, which can protect the existence of gapless nodal ring in $k_z = 0$ plane with respect to SOC [15, 28] [see Fig. 2(b)]. The topological invariant of the nodal ring can be viewed as the variation of the quantized Berry phase with respect to the mirror plane [47], which is related to the change at the end of the one-dimensional system along a line across the ring in $k_z = 0$ plane. As shown in Fig. 3(a), the Berry phase of β - V_2OPO_4 shows the jump across the ring, further confirming the topological features of the nodal ring perpendicular to the [001] magnetization direction.

Our calculations suggest that the magnetization along other directions is energetically very close to the [001]. When the magnetization is deviated from [001] direction, the mirror reflection symmetry is broken. Here, we take the case of [110] magnetization as an example since the symmetry analysis for the rest cases are essentially the same. The group elements of the corresponding magnetic space group C_{2h} remains: I , C_2^{110} and TC_2^z , $TC_2^{1\bar{1}0}$. The vanishing of mirror reflection symmetry makes nodal line gapped. However, the anti-unitary symmetry TC_2^z allows the existence of Weyl points in $k_z = 0$ plane. A pair of Weyl points protected by the C_2^{110} rotation is present on $k_x = k_y$ axis.

We also calculate the parities of inversion eigenvalues at time reversal invariant momenta (TRIM) points. The product of the occupied bands running over all TRIM points is -1, confirming the presence of odd number of pairs of Weyl points [48]. As shown in Fig. 2(b), the two crossing bands along Γ -X (or [110]) belong to eigenvalues $\pm i$ of C_2^{110} , respectively. The chirality of Weyl point can be determined by the evolution of the average position of Wannier centers, and the Wilson-loop method applied on a sphere around a Weyl point is used [49, 50] [see Fig. 3(b)]. The Weyl point with Chern number $C = +1$ is located at $(0.46\text{\AA}^{-1}, 0.46\text{\AA}^{-1}, 0)$ in momentum space, while the Weyl point with Chern number $C = -1$ related by I symmetry located at same axis [see Fig. 1(c)]. The Weyl points only existed on $k_x = k_y$ axis can be further verified by the Berry curvature. As shown in Fig. 3(c), the Weyl points with positive and negative chirality are regarded as the "source" and "sink" of Berry curvature in momentum space.

As it is discussed above, our results indicate the existence of either the topological NLs or WSMS in FM β - V_2OPO_4 compound, depending on the magnetization direction. The NL features are protected by the mirror reflection symmetry in the case of [001] magnetization,

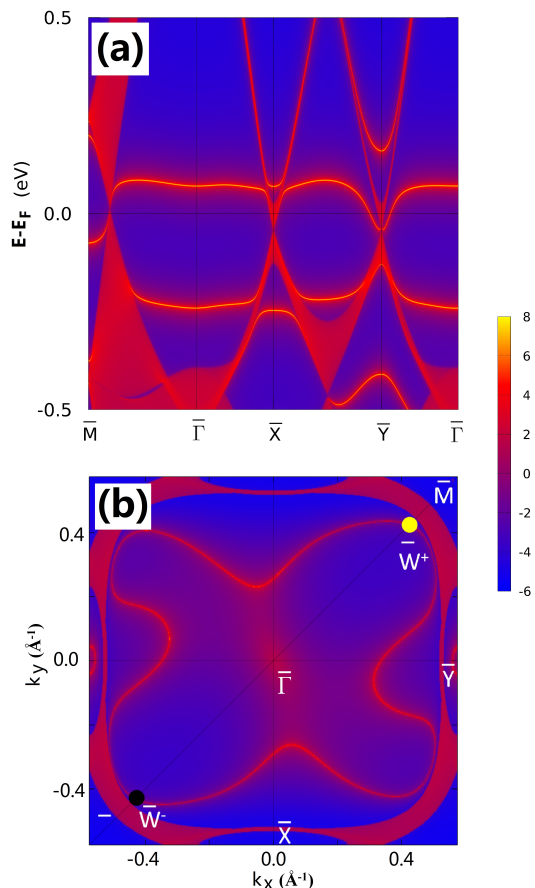


FIG. 4. The surface states and Fermi surfaces. (a) The surfaces projected on (001) surfaces. (b) The corresponding Fermi surfaces on (001) surfaces. The projected Fermi surface is calculated with a chemical potential of 60 meV.

while the WSM features can arise with magnetization direction along other high symmetry axis. The Weyl points would be protected by C_2^m rotational symmetry, where m represents a symmetry axis in $x-y$ plane. In the cases of which only a pair of Weyl points, the minimum number of Weyl points in condensed matter systems, with large separation in momentum. Considering the energy of Weyl points in FM β - V_2OPO_4 is very close to Fermi level, e.g. ~ 12 meV when [110] magnetization, we would suggest β - $VOPO_4$ compound to be an excellent experimental candidate for the observation of the nontrivial properties in FM WSMs.

One hallmark of nontrivial semimetals is the existence of topologically protected surface state, which arises from the inversion of TRIM parities. In the WSM states, topological surface bands connect the valence and conduction bands. The drumhead surface states of NLSs

will appear when the gap of bulk band is closed forming a nodal ring. Since the gap size of WSM state is very small, which make only tiny difference of surface states between NL and WSM phases. Here, we only present the surface states and Fermi arcs in the [110] magnetic configuration. To obtain the surface states, we constructed a tight-binding (TB) Hamiltonian with basis of maximally localized Wannier functions [44, 45] in which the Green's function method [51] is employed. The calculated local density of states (LDOS) and Fermi surface projected on (001) surface are shown in Figs. 4(a) and (b), respectively. The surface states are clearly observed in Fig. 4(a). On the (001) surface, the anti-unitary magnetic symmetry TC_2 leads to different behavior for the surface bands around the \bar{X} and \bar{Y} . Although some trivially residual bands would project on (001) surface of this compound, the Fermi arc states are quite clear as it is shown in Fig. 4(b).

In conclusion, using first-principles calculations, we proposed that FM vanadium-phosphorous-oxide β - V_2OPO_4 can possess the nontrivial properties of TSMs, either NLs or WSMs, that can be switched between each other by different magnetization directions. When the spin is polarized along [001] direction, system belongs to $D_{4h}(C_{4h})$ point group and present the gapless nodal ring, protected by the mirror reflection symmetry, close to the Fermi level at $k_x - k_y$ plane with $k_z = 0$ in momentum space. When the magnetization directions deviate from [001], the nodal ring will degenerate to a pair of Weyl points due to the vanishing of mirror reflection symmetry. These two Weyl points, protected by twofold rotational symmetry along magnetization directions, lie in $k_x - k_y$ plane with $k_z = 0$, which are largely separated in momentum. All the non-trivial band-crossing points are very close to the Fermi level. The topology of the system is confirmed by the existence of non-trivial surface states. Since β - V_2OPO_4 has been fabricated for years [46], our proposition provides a realistic and promising candidate for the investigation of magnetic TSMs in experiments, particularly towards the realization of quantum anomalous Hall effect condensed matter systems.

Acknowledgments– This work is supported by the National Natural Science Foundation of China (NSFC, Grant Nos.11204185, 11304403, 11334003 and 11404159).

AUTHOR INFORMATION

*Equal Contributions:

Y. J. Jin and R. Wang contributed equally to this work.

†Corresponding author:

xuh@sustc.edu.cn (H.X.)

-
- [1] E. H. Hall, *Am. J. Math.* **2**, 287 (1879).
- [2] K. Klitzing, G. Dorda, and M. Pepper, *Phys. Rev. Lett.* **45**, 494 (1980).
- [3] D. C. Tsui, H. L. Stormer, and A. C. Gossard, *Phys. Rev. Lett.* **48**, 1559 (1982).
- [4] S. Murakami, N. Nagaosa, and S. C. Zhang, *Science* **301**, 1348 (2003).
- [5] B. A. Bernevig, T. L. Hughes, and S. C. Zhang, *Science* **314**, 1757 (2006).
- [6] M. König, S. Wiedmann, C. Brüne, A. Roth, H. Buhmann, L. W. Molenkamp, X. L. Qi, and S. C. Zhang, *Science* **318**, 766 (2007).
- [7] X. L. Qi, Y. S. Wu, and S. C. Zhang, *Phys. Rev. B* **74**, 085308 (2006).
- [8] R. Yu, W. Zhang, H. Zhang, S. C. Zhang, X. Dai, and Z. Fang, *Science* **329**, 61 (2010).
- [9] C. Z. Chang, et. al., *Science* **340**, 167 (2013).
- [10] C. Fang, M. J. Gilbert, and B. A. Bernevig, *Phys. Rev. Lett.* **112**, 046801 (2014).
- [11] C. Z. Chang, et. al., *Nature Materials*, **14**, 473 (2015).
- [12] G. Xu, H. Weng, Z. Wang, X. Dai, and Z. Fang, *Phys. Rev. Lett.* **107**, 186806 (2011).
- [13] X. Wan, A. M. Turner, A. Vishwanath, and S. Y. Savrasov, *Phys. Rev. B* **83**, 205101 (2011).
- [14] A. A. Burkov, M. D. Hook, and L. Balents, *Phys. Rev. B* **84**, 235126 (2011).
- [15] H. Weng, C. Fang, Z. Fang, B. A. Bernevig, and X. Dai, *Phys. Rev. X* **5**, 011029 (2015).
- [16] S.-M. Huang, S.-Y. Xu, I. Belopolski, C.-C. Lee, G. Chang, B. Wang, N. Alidoust, G. Bian, M. Neupane, C. Zhang, S. Jia, A. Bansil, H. Lin, and M. Z. Hasan, *Nat. Commun.* **6**, 7373 (2015).
- [17] J. Ruan, S.-K. Jian, H. Yao, H. Zhang, S.-C. Zhang, and D. Xing, *Nat. Commun.* **7**, 11136 (2016).
- [18] J. Ruan, S.-K. Jian, D. Zhang, H. Yao, H. Zhang, S.-C. Zhang, and D. Xing, *Phys. Rev. Lett.* **116**, 226801 (2016).
- [19] G. Autès, D. Gresch, M. Troyer, A. A. Soluyanov, and O. V. Yazyev, *Phys. Rev. Lett.* **117**, 066402 (2016).
- [20] Z. Wang, D. Gresch, A. A. Soluyanov, W. Xie, S. Kushwaha, X. Dai, M. Troyer, R. J. Cava, and B. A. Bernevig, *Phys. Rev. Lett.* **117**, 056805 (2016).
- [21] Y. Xu, C. Yue, H. Weng, and X. Dai, *Phys. Rev. X* **7**, 011027 (2017).
- [22] S.-Y. Xu, I. Belopolski, N. Alidoust, M. Neupane, G. Bian, C. Zhang, R. Sankar, G. Chang, Z. Yuan, C.-C. Lee, S.-M. Huang, H. Zheng, J. Ma, D. S. Sanchez, B. Wang, A. Bansil, F. Chou, P. P. Shibayev, H. Lin, S. Jia, and M. Z. Hasan, *Science* **349**, 613 (2015).
- [23] B. Q. Lv, H.M. Weng, B. B. Fu, X. P. Wang, H. Miao, J. Ma, P. Richard, X. C. Huang, L. X. Zhao, G. F. Chen, Z. Fang, X. Dai, T. Qian, and H. Ding, *Phys. Rev. X* **5**, 031013 (2015).
- [24] L. X. Yang, Z. K. Liu, Y. Sun, H. Peng, H. F. Yang, T. Zhang, B. Zhou, Y. Zhang, Y. F. Guo, M. Rahn, D. Prabhakaran, Z. Hussain, S. K. Mo, C. Felser, B. Yan, and Y. L. Chen, *Nat. Phys.* **11**, 728 (2015).
- [25] A. Tamai, Q. S. Wu, I. Cucchi, F. Y. Bruno, S. Riccò, T. K. Kim, M. Hoesch, C. Barreateau, E. Giannini, C. Besnard, A. A. Soluyanov, and F. Baumberge, *Phys. Rev. X* **6**, 031021 (2016).
- [26] J. Liu and D. Vanderbilt, *Phys. Rev. B* **90**, 155316 (2014).
- [27] D. Bulmash, C.-X. Liu, and X.-L. Qi, *Phys. Rev. B* **89**, 081106(R) (2014).
- [28] Z. Wang, M. G. Vergniory, S. Kushwaha, M. Hirschberger, and E. V. Chulkov, *Phys. Rev. Lett.* **117**, 236401 (2016).
- [29] E. Benser, R. Glaum, T. Dross, and H. Hibst, *Chem. Mater.* **19**, 4341 (2007).
- [30] M. Satyanarayana, R. S. Rao, V. Pralong, and U. V. Varadaraju, *J. Electrochem. Soc.* **164** A6201 (2017).
- [31] G. Kresse and J. Furthmüller, *Phys. Rev. B*, **54**, 11169 (1996).
- [32] G. Kresse and J. Furthmüller, *Comput. Mater. Sci.* **6**, 15 (1996).
- [33] P. Hohenberg and W. Kohn, *Phys. Rev.* **136**, B864 (1964).
- [34] W. Kohn, L. J. Sham, *Phys. Rev.* **140**, A1133 (1965).
- [35] J. P. Perdew, K. Burke, M. Ernzerhof, *Phys. Rev. Lett.* **77**, 3865 (1996).
- [36] J. P. Perdew, K. Burke, M. Ernzerhof, *Phys. Rev. Lett.* **78**, 1396 (1996).
- [37] P. E. Blöchl, *Phys. Rev. B* **50**, 17953 (1994).
- [38] G. Kresse, D. Joubert, *Phys. Rev. B* **59**, 1758 (1999).
- [39] D. M. Ceperley and B. J. Alder, *Phys. Rev. Lett.* **45**, 566 (1980).
- [40] H. J. Monkhorst, J. D. Pack, *Phys. Rev. B* **13**, 5188 (1976).
- [41] A. I. Liechtenstein, V. I. Anisimov and J. Zaane, *Phys. Rev. B* **52** 5467 (R) (1995).
- [42] M. A. Korotin, V. I. Anisimov, D. I. Khomskii, and G. A. Sawatzky, *Phys. Rev. Lett.* **80**, 4305 (1998).
- [43] A. Liebsch, H. Ishida, and G. Bihlmayer, *Phys. Rev. B* **71** 085109 (2005).
- [44] N. Marzari, A. A. Mostofi, J. R. Yates, I. Souza, and D. Vanderbilt, *Rev. Mod. Phys.* **84**, 1419 (2012).
- [45] A. A. Mostofi, J. R. Yates, Y. S. Lee, I. Souza, and D. Vanderbilt, and N. Marzari, *Comput. Phys. Commun.* **178**, 685 (2008).
- [46] R. Glaum and R. Gruehn, *Zeitschrift fuer Krist.* **186**, 91 (1989).
- [47] D. Vanderbilt and R. D. King-Smith, *Phys. Rev. B* **48**, 4442 (1993).
- [48] T. L. Hughes, E. Prodan, and B. A. Bernevig, *Phys. Rev. B* **83**, 245132 (2011).
- [49] R. Yu, X. L. Qi, A. Bernevig, Z. Fang, and X. Dai, *Phys. Rev. B* **84**, 075119 (2011).
- [50] A. A. Soluyanov and D. Vanderbilt, *Phys. Rev. B* **83**, 035108 (2011).
- [51] M. P. López Sancho, J. M. López Sancho, and J. Rubio, *J. Phys. F* **14**, 1205 (1984); **15**, 851 (1985).

Supplemental Material for
“Topological Semimetals in
Ferromagnetic
Vanadium-Phosphorous-Oxide β -V₂OPO₄
Compound”

I. TWO-BAND 2×2 $k \cdot p$ HAMILTONIAN

In the absence of SOC, a node-line around the Γ point in $k_z = 0$ plane is present. Generally, the nodal ring around the Γ point can be modeled by a two-band $k \cdot p$ theory, and the Hamiltonian is

$$H = \sum_{i=x,y,z} d_i(\mathbf{k})\sigma_i, \quad (\text{S1})$$

where $d_i(\mathbf{k})$ are real functions and $\mathbf{k} = (k_x, k_y, k_z)$ are three components of the momentum \mathbf{k} relative to the Γ point. In Eq. (S1), we have ignored the kinetic term proportional to the identity matrix, since it is irrelevant in studying the band crossing. The Pauli matrix σ_i are

$$\sigma_x = \begin{pmatrix} 0 & 1 \\ 1 & 0 \end{pmatrix}, \sigma_y = \begin{pmatrix} 0 & -i \\ i & 0 \end{pmatrix}, \sigma_z = \begin{pmatrix} 1 & 0 \\ 0 & -1 \end{pmatrix} \quad (\text{S2})$$

Within SOC, two spin channels couple together and symmetries can decrease depending on the direction of the spontaneous magnetization. In spin representation, an any three dimensional (3D) rotation $R(\alpha, \beta, \gamma)$ has to correspond a two-dimensional (2D) unitary matrix $u(\alpha, \beta, \gamma)$ as

$$u(\alpha, \beta, \gamma) = \begin{pmatrix} e^{-i\frac{\alpha+\gamma}{2}} \cos \frac{\beta}{2} & -e^{-i\frac{\alpha-\gamma}{2}} \sin \frac{\beta}{2} \\ e^{i\frac{\alpha-\gamma}{2}} \sin \frac{\beta}{2} & e^{i\frac{\alpha+\gamma}{2}} \cos \frac{\beta}{2} \end{pmatrix}, \quad (\text{S3})$$

where α, β, γ are Euler angle of 3D rotation.

II. THE NODAL RING DEPENDING ON
MAGNETIC SPACE GROUP $D_{4h}(C_{4h})$ IN THE
PRESENCE OF SPIN-ORBITAL-COUPLING

When all spins are oriented along $[011]$ (or z) direction, the C_{4h} subgroup of D_{4h} is just the fourfold rotation group C_4^z with respect to z coordinate axis tensored by the inversion I , namely $C_4^z \otimes I$. With $[100]$ magnetization, the group elements of the corresponding magnetic space group $D_{4h}(C_{4h})$ remains: $I, C_{4x}, C_2^z \cdot I, C_2^{010} \cdot T$, and $C_2^{100} \cdot T$. It is important note that the product $C_2^z \cdot I$ of twofold rotation C_2^z and inversion I is mirror-reflection symmetry M_z with respect to (001) plane. The matrix form of M_z in spin representation is

$$C_2^z \cdot I = \begin{pmatrix} e^{i\frac{\pi}{2}} & 0 \\ 0 & e^{-i\frac{\pi}{2}} \end{pmatrix} = i\sigma_z. \quad (\text{S4})$$

The mirror reflection indicates the Hamiltonian in xy [or (001)] plane as

$$H(k_x, k_y, 0) = \sigma_z H(k_x, k_y, 0) \sigma_z \quad (\text{S5})$$

or

$$\begin{aligned} d_x(k_x, k_y, 0) &= -d_x(k_x, k_y, 0) \equiv 0, \\ d_y(k_x, k_y, 0) &= -d_y(k_x, k_y, 0) \equiv 0, \end{aligned} \quad (\text{S6})$$

The energy dispersion of the two-band Hamiltonian with $C_2^z \cdot I$ symmetry is

$$E = \pm |d_z(k_x, k_y, 0)|. \quad (\text{S7})$$

Generically, the band crossing means $d_z(k_x, k_y, 0) = 0$, which has codimension one, i.e., a nodal loop solution in xy plane.

III. THE WEYL POINTS DEPENDING ON
MAGNETIC SPACE GROUP $D_{4h}(C_{2h})$ IN THE
PRESENCE OF SPIN-ORBITAL-COUPLING

We show that the Weyl points can arise with magnetization direction along high symmetry axis, as long as the magnetic space group C_{2h} symmetry remains. The Weyl points are protected by C_2^m rotation, where m represents a symmetry axis in xy [or (001)] plane. As a example, we mainly show the case of magnetization along $[100]$ axis.

With $[100]$ magnetization, the group elements of the corresponding magnetic space group $D_{4h}(C_{2h})$ remains: $I, C_2^z \cdot T, C_2^{010} \cdot T$, and C_2^{100} . We now analyze the group elements on different axes to find out if Weyl points can arise generically on those axes in (001) plane. Firstly, we prove the product $C_2^z \cdot T$ of time reversal $T = -i\sigma_y K$ and rotation C_2^z allowing for the existence of Weyl points in the (110) plane. The anti-unitary $C_2^z \cdot T$ with matrix representation is

$$\begin{aligned} C_2^z \cdot T &= i \begin{pmatrix} e^{-i\frac{\pi}{2}} & 0 \\ 0 & e^{i\frac{\pi}{2}} \end{pmatrix} \begin{pmatrix} 0 & -i \\ i & 0 \end{pmatrix} K \\ &= i\sigma_x K, \end{aligned} \quad (\text{S8})$$

with complex conjugation K . The anti-unitary $C_2^z \cdot T$ requires the commutation relation as

$$[H, C_2^z \cdot T] = [H, i\sigma_x K] = 0, \quad (\text{S9})$$

i.e.,

$$\begin{aligned} d_x(k_x, k_y, 0)[\sigma_x, i\sigma_x K] + d_y(k_x, k_y, 0)[\sigma_y, i\sigma_x K] \\ + d_z(k_x, k_y, 0)[\sigma_z, i\sigma_x K] = 0, \end{aligned} \quad (\text{S10})$$

which gives

$$d_z(k_x, k_y, k_z) \equiv 0. \quad (\text{S11})$$

Now the Hamiltonian in (001) plane is

$$H = d_x(k_x, k_y, 0)\sigma_x + d_y(k_x, k_y, 0)\sigma_y. \quad (\text{S12})$$

It is noted that the Hamiltonian contains two parameters and two momenta. Hence the crossing points can generically exist in the (001) plane.

In the following, we show that the Weyl points can arise from the unitary element C_2^{100} with [100] magnetization axis. This symmetry requires the constraints:

$$[H, C_2^{100}] = 0. \quad (\text{S13})$$

In spin representation, the unitary matrix C_2^{100} can be obtained Eq. (S3), as

$$C_2^{100} = \begin{pmatrix} 0 & i \\ i & 0 \end{pmatrix} = i\sigma_x. \quad (\text{S14})$$

Eq. (S13) gives

$$H(k_x, k_y, 0) = \sigma_x H(k_x, -k_y, 0)\sigma_x \quad (\text{S15})$$

or

$$\begin{aligned} d_x(k_x, k_y, 0) &= d_x(k_x, -k_y, 0), \\ d_y(k_x, k_y, 0) &= -d_y(k_x, -k_y, 0). \end{aligned} \quad (\text{S16})$$

In $k_y = 0$ axis, i.e. [100] direction, Eq. (S16) must requires

$$d_y(k_x, 0, 0) \equiv 0. \quad (\text{S17})$$

The energy dispersion of the two-band Hamiltonian after considering C_2^{100} symmetry is

$$\begin{aligned} E &= \pm \sqrt{d_x(k_x, k_y, 0)^2 + d_y(k_x, k_y, 0)^2} \\ &= \pm |d_x(k_x, 0, 0)|. \end{aligned} \quad (\text{S18})$$

In low-energy case, we have

$$d_x(k_x, 0, 0) = A + Bk_x + Ck_x^2 + \dots, \quad (\text{S19})$$

and then the zero energy mode can require a pair of Weyl points locate at $k_x = \pm k_x^c$ when $B = 0$ and $AC < 0$. Two bands with eigenvalues $\pm i$ of C_2^{100} can cross on this axis. Along other direction with $k_y = ak_x$ through Γ point on the xy plane, the Hamiltonian contains two function d_x and d_y , but one momentum k_x , indicating that there are no Weyl points on the $k_y = ak_x$ line. Hence, the crossing would splits away from [100] axis. Similarly, when magnetization is along [110], [010], and $[1\bar{1}0]$ directions, the Weyl points also arise due to C_2^m rotation of magnetic space group $D_{4h}(C_{2h})$. The Weyl points are only allowed in m axis.